euspen's 20th International Conference & Exhibition, Geneva, CH, June 2020
www.euspen.eu

Master select control method for parallel-connected dual PMSMs fed by a single inverter in hydraulic driver system of machine tools

Chul Yun[1], Taeho Oh[1], Jooyong Park[1], Taesung Jang[1], Nakwon Choi[1], Seongdae Kim[1], Myongsu Oh[1] and Naesoo Cho[2]

[1]*Doosan Machine Tools*, [2]*Keimyung College University*

chul.yun@doosanmt.com , *taeho.oh1@doosanmt.com* , *jooyong.park@doosanmt.com* , *taesung.jang@doosanmt.com* , *nakwon.choi@doosanmt.com* , *seongdae.kim@doosanmt.com* , *myungsu.oh@doosanmt.com* , *nascho@kmuc.ac.kr*

Abstract
In the hydraulic system field of machine tools, an energy-saving hydraulic system composed of an inverter capable of efficiently operating a plurality of motors is used for various applications such as a clamping operation. However, if the motor is added, the inverter is added together, which increases the cost. To compensate for this drawback, This paper proposes a master select control method for parallel-connected dual Permanent Magnet Synchronous Motors (PMSMs) fed by a single inverter in hydraulic driver system of machine tools. Unlike conventional algorithms, the proposed algorithm does not need speed sensor and hysteresis comparator, which are required in the averaged energy and rotor position error methods. The algorithm directly chooses the master motor with direct measured flux-axis current so that the dynamic characteristic in sensorless speed control is faster than that of the conventional methods. The results of simulation conducted verify the efficacy of the proposed method.

Keywords : SIMM, Master select control, Hydraulic system

1. Introduction

In the hydraulic system field of machine tools, an energy-saving hydraulic system composed of an inverter capable of efficiently operating a plurality of motors is used for various applications such as a clamping operation. The hydraulic system are generally required to operate in a dwelling state to efficiently save energy. In response to these demands, recent industrial sites use energy-saving hydraulic systems composed of high efficiency motors and inverters.

However, due to the addition of the power semiconductor and the control element according to the use of the inverter for each motor, there is a disadvantage that the cost of adding the inverter compared to the existing constant speed induction motor. This paper proposes a master select control method for parallel-connected dual Permanent Magnet Synchronous Motors (PMSMs) fed by a single inverter in hydraulic driver system of machine tools. Unlike conventional algorithms, the proposed algorithm does not need speed sensor and hysteresis comparator, which are required in the averaged energy and rotor position error methods. The algorithm directly chooses the master motor with direct measured flux-axis current so that the dynamic characteristic in sensorless speed control is faster than that of the conventional methods. The results of simulation conducted verify the efficacy of the proposed method. Accordingly, in order to drive multiple SPMSM(Surface-mounted Permanent Magnet Synchronous Motors)s via multiple inverters rotor position detection sensors are required. This increases the overall product size, volume, and production costs. To solve this problem, several methods for driving multiple motors with a single inverter, as shown in Figure. 1, have been proposed [1]-[6].

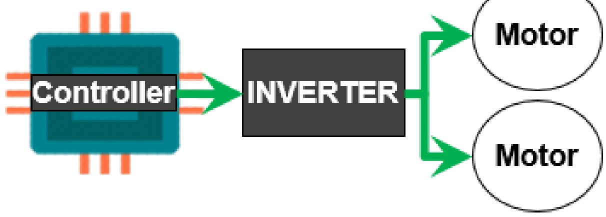

Figure 1. Structure of a Single Inverter Multi-Motor (SIMM) system

2. Dynamic stability analysis by the torque angle

The principle of power occurrence can be physically determined from the flux relationship by drawing a vector diagram such as that shown in Figure 2.

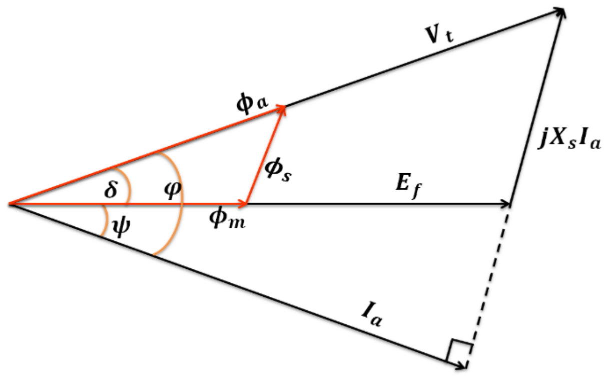

Figure 2. SPMSM vector diagram

In Figure 2, V_t is the armature voltage, I_a is the armature current, E_f is the excitation voltage, X_s is the synchronous reactance, ϕ_a is the air-gap flux, ϕ_m is the permanent magnet flux, ϕ_s is the armature reaction flux, φ is the power factor angle between V_t and I_a , ψ is the inner power angle between I_a and , and E_f, and δ is the torque or power angle between V_t and E_f .

In below equations, P is the input power, ω_{rm} is the angular velocity, T is the mechanical output torque.
The input power can be derived as equation (1) from the vector diagram:

$$P = 3V_t I_a cos\varphi \tag{1}$$

The armature current can be found from equation (2):

$$I_a cos\varphi = \frac{E_f sin\delta}{X_s} \tag{2}$$

Equation (3) shows the mechanical output torque of the output power, found by substituting equation (2) into equation (1).

$$T = \frac{P}{\omega_{rm}} = 3\frac{V_t E_f sin\delta}{\omega_{rm} X_s} = T_{max} sin\delta \tag{3}$$

Equation (3) expresses the voltage and excitation voltage. Compared with the vector diagram, the excitation voltage vector direction is the same as that of the permanent magnetic flux and the vector direction of the voltage is identical to the air-gap flux direction. Therefore, the maximum torque can be controlled by the excitation voltage when the voltage is kept constant. Figure 3 illustrates equation (3) according to torque angle.

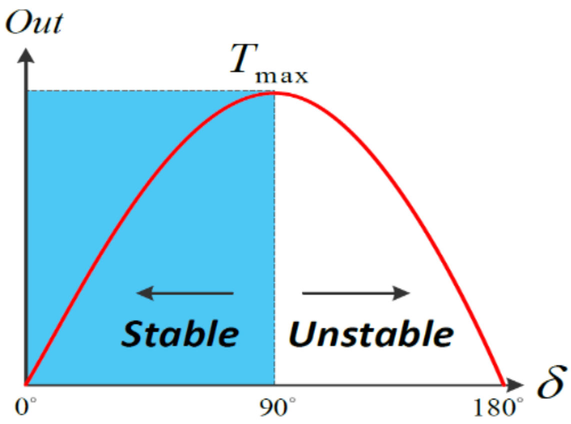

Figure 3. Torque property according to $\boldsymbol{\delta}$

Output torque is determined by δ in the constant torque region, in which the voltage and excitation voltage area is fixed, as shown in Figure 3. The maximum torque occurs at $\delta = 90°$. If the torque angle is $90° < \delta < 180°$, the torque will lose the acceleration and the motor will be divergent [7].

3. Load torque recognition method by flux-axis current

A vector diagram of a typical parallel-connected SPMSM at disagreement load state is depicted in Figure 4 [3][4]. The master motor is selected by relation between excitation voltage and flux position. In Figure 4, M1 is the master motor and M2 is the slave motor. Because the load torque of M2 is greater than that of M1, $\delta_1 < \delta_2$ in Figure 4(a). Conversely, in Figure 4(b), because the load torque of M2 is smaller than that of M1, $\delta_1 > \delta_2$.

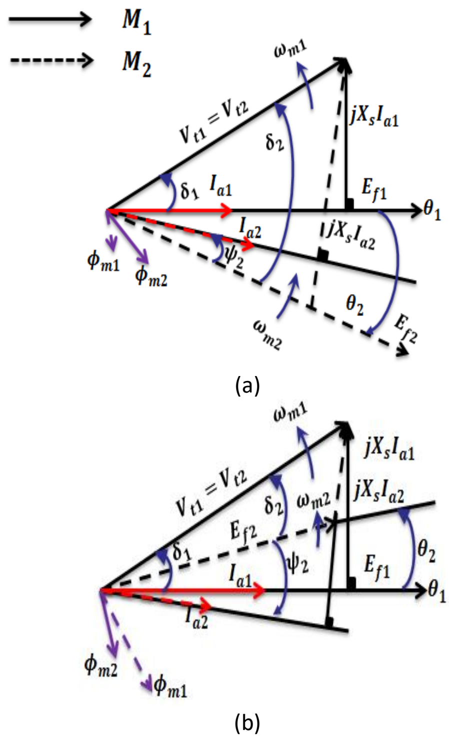

Figure 4. Parallel connected SPMSM vector diagram: (a) Case 1: $T_{L1} < T_{L2}$, (b) Case 2: $T_{L1} > T_{L2}$

From equations The torque-axis voltage and the flux-axis voltage, the torque-axis current and flux-axis current can be expressed as equation (4):

$$\begin{aligned} I_d &= I_a sin(\varphi - \delta) \\ I_q &= I_a cos(\varphi - \delta) \end{aligned} \tag{4}$$

where, I_d is the flux-axis current and I_q is the torque-axis current. When the torque angle increases, the flux-axis current rises in the negative direction and the torque-axis current decreases, as shown in equation (4). It collapses the dynamic stability limit load torque. Therefore, in this paper, the load change is recognized by comparing the flux-axis current between the two motors.

$$\begin{aligned} \Delta i_d^r &= i_{d_{m1}}^r - i_{d_{m2}}^r \\ sgn(\Delta i_d^r) &= \begin{Bmatrix} 1 \ (\Delta i_d^r > 0) \\ -1 \ (\Delta i_d^r < 0) \end{Bmatrix} \end{aligned} \tag{5}$$

First, the error between the flux-axis current measured from the two motors is calculated using equation (5). The output of the sign function is 1 when the error is positive, otherwise the output is -1. Thus, it is possible to select the feedback value control of the controller based on the sign function output. As a result, the controller controls the heavy load motor along with the sign function result, as shown in Figure 5. On the other hands, if the load of master motor is bigger than slave one, the output of sign function is positive but slave one is bigger than the master motor then sign function output is negative by equation (5). As a result of that motor which has bigger load can be controlled by sign function output. Since the control motor is selected using flux-axis current, it can be applied to the sensorless system, and faster dynamic property can be obtained in load alteration because actual measured current is being used.

In Figure 5, ω_r is the angular velocity of motors, θ_r is the position of motors.

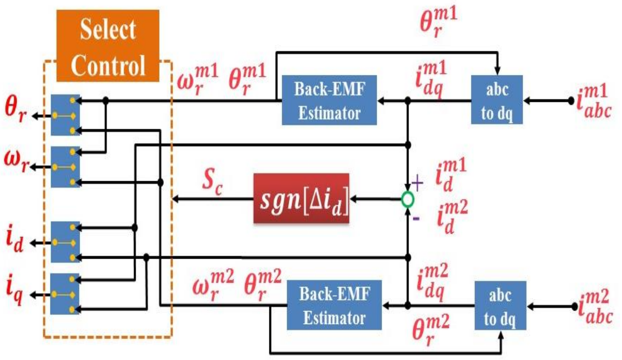

Figure 5. Select control block diagram

4. Simulation results

To verify the efficacy of the proposed method, parallel sensorless speed control system fed by a single inverter using SPMSMs flux-axis current, we simulated the algorithm. The sensorless speed control algorithm simulated estimates the rotor position and speed by back-EMF estimator using motor current. The simulation considered both steady-state and dynamic state characteristics.

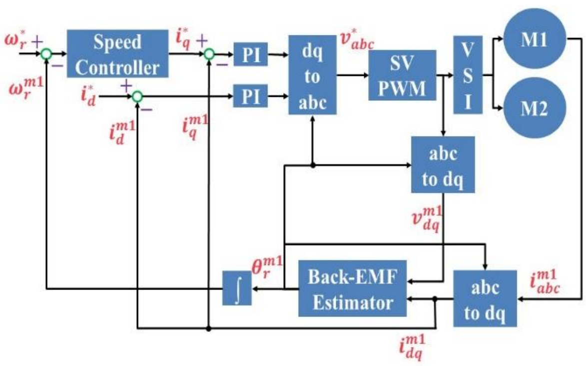

Figure. 3. SIMM structure without select control

First of all, torque angle and flux-axis current were observed so as to check the dynamic property of the parallel drive without select control, as shown in Figure 6, by inserting load to M2.

Next, as indicated in Figure 7, the dynamic characteristics of the proposed system, which has select control for parallel drive, were confirmed in like manner. The simulation was conducted using MATLAB/SIMULINK and the commonly used PI controller composed for current control. Voltage was modulated by a space vector PWM inverter, and rotor position, and speed information obtained from the back-EMF estimator. As shown in Figure 5 and equation (10), select control by flux-axis current is realized. Table 1 shows the SPMSM parameters.

Table 1. Nominal parameters for 26 W SPMSM

Base Speed	4000 rpm
R_s	0.6 Ω
L_s	0.17 mH
T_L	0.062 N.m
ϕ_m	0.0035 Wb
poles	8

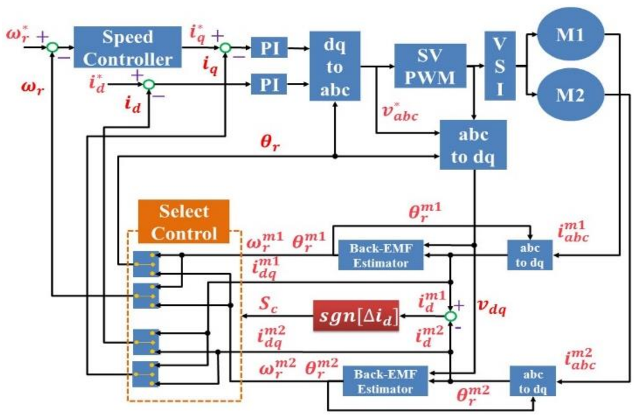

Figure. 4. Block diagram of the proposed system

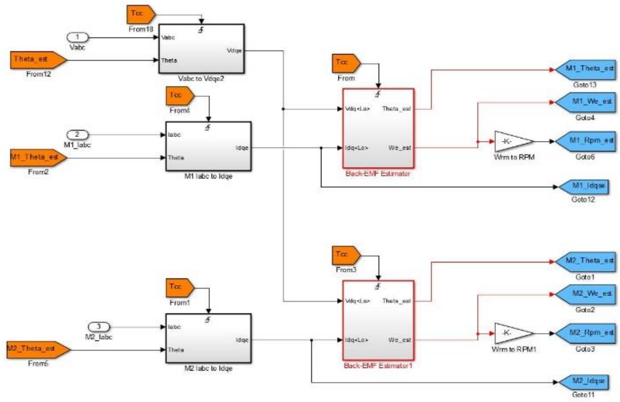

Figure. 5. Block diagram for sensorless algorithm

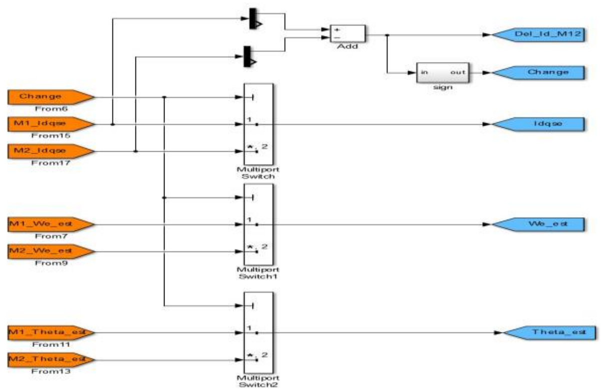

Figure. 6. Selection control block diagram

Figure 8 shows the block diagram for sensorless algorithm. Reference voltage is calculated with master motor rotating position for coordinate conversion since this paper controls only the master motor. However reference frame transformation for current uses the rotor positon of each motor.

Figure 9 indicates the way to choose the master motor from d-axis current.

Motors simultaneously drive with rated speed command at 4000 rpm between 0–0.3 s in no-load condition. In the structure of the proposed method, illustrated in Figure 10, the rated load torque is applied to only M2 at 0.6 s to verify the speed response in asynchronous load conditions for the motors to accelerate up to a rated speed of 4000 rpm between 0–0.3s.

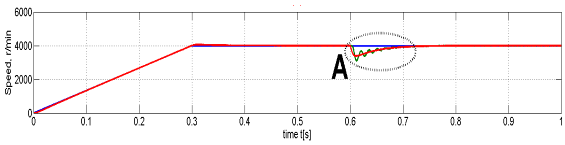

(a)

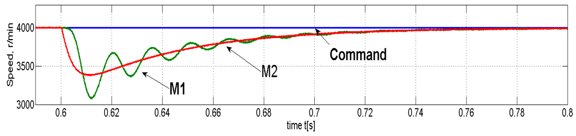

(b)

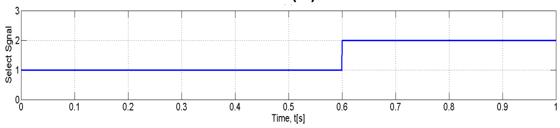

(c)

Figure 10. Speed response in unbalanced load:
(a) Speed response, (b) Zoom in region A, (c) Select signal

Figure 10(b) shows the enlargement region A (around 0.6 s) of Figure 10(a), while Figure 10(c) illustrates the select signal by load change. At the transient state by load fluctuation, M1 speed vibrates around M2 speed and both motors become stable at the specified speed in 0.7 s, as shown in Figure 10(b). A stable select signal occurs by comparing the flux-axis current about the unbalanced load from Figure 10(c).

5. Conclusion

This paper proposes a master select control method for parallel-connected dual SPMSMs fed by a single inverter in hydraulic driver system of machine tools. The proposed algorithm compares the flux-axis current of each motor, and detects the control signal from the relation between the back-EMF for torque angle and current by unbalanced load oscillation.

Unlike conventional algorithms, the proposed algorithm does not need speed sensor and hysteresis comparator, which are required in the averaged energy and rotor position error methods. The algorithm directly chooses the master motor with direct measured flux-axis current so that the dynamic characteristic in sensorless speed control is faster than that of the conventional methods.

Further, the proposed algorithm is able to stably drive the overall load torque area. It has the advantage of reduced computation because it uses only one speed controller. Finally, we verified that the proposed algorithm enables motors connected in parallel to operate stably during asynchronous load fluctuations and high frequency load change conditions via simulations with MATLAB/SIMULINK and experiment with a three-phase inverter system.

References

[1] A. Asri, D. Ishak, S. Iqbal, M. Kamarol, 2011 ICCSCE. IEEE International Conference on Control System. 567-570

[2] A. A. A. Samat, D. Ishak, P. Saedin, and S. Iqbal, 2012 IEEE International Power Engineering and Optimization Conference. 35-39

[3] J. Matlagi, Z. Ibrahim, M. Sulaiman, 2011 Journal of Theoretical and Applied information Technology. *Vol*. **33** 76-82

[4] J. M. Lazi, Z. Ibrahim, M. H. N. Talib, R. Mustafa, 2010 PECon IEEE International Conference on Power and Energy. 786-790

[5] D. Bidart, M. Pietrzak-David, P. Maussion, M. Fadel 2008 IECON 34th Annual Conference of IEEE. 268-273

[6] D. Bidart, M. Pietrzak-David, P. Maussion, M. Fadel 2011 IET. Electric Power Applications. *Vol.* **5** 288-294

[7] P. C. Sen, “Principles of electric machines and power electronics Second Edition”, John Wiley&Sons, 9/ pp. 479-493, 1998